N-heterocyclic carbene-stabilized Au_{13} superatom clusters

Mina R. Narouz[†], Shinjiro Takano[¶], Paul A. Lummis[†], Tetyana I. Levchenko[†], Ali Nazemi[†], Sami Kaappa[fl], Sami Malola[fl], Seyedehgoonay Yousefalizadeh[†], Kevin G. Stamplecoskie[†*], Hannu Häkkinen[fl]*, Tatsuya Tsukuda[¶§]* and Cathleen M. Crudden[†‡]*

[†]Department of Chemistry, Queen's University, Chernoff Hall, Kingston, Ontario, Canada, K7L 3N6 [¶]Department of Chemistry, School of Science, The University of Tokyo, 7-3-1 Hongo, Bunkyo-ku, Tokyo 113-0033, Japan [§]Elements Strategy Initiative for Catalysts and Batteries (ESICB), Kyoto University, Katsura, Kyoto 615-8520, Japan [fl]Departments of Chemistry and Physics, Nanoscience Center, University of Jyväskylä, 40014 Jyväskylä, Finland [‡]Institute of Transformative Bio-Molecules (WPI-ITbM), Nagoya University, Chikusa, Nagoya, Japan, 464-8602.

Supporting Information Placeholder

ABSTRACT: Magic number Au_{13} nanoclusters stabilized entirely by N-heterocyclic carbenes (NHCs) have been prepared by the bottom-up reduction of well-defined molecular NHC–Au–Cl complexes with sodium borohydride. The nature of the wingtip groups was shown to be critical in the preparation of stable clusters. The all NHC-clusters are prepared in high yield by this straightforward method, display higher stability than related all phosphine clusters, and possess extremely high emission quantum yield. DFT analysis of these clusters based on the resolved crystal structure reveals their electronic structure as 8-electron superatoms.

Metal nanoclusters are atomically-precise class of nanomaterials that, unlike metal nanoparticles, feature precise structures and discrete molecular orbitals and electronic transitions.[1] Since the ground-breaking report from Kornberg of a crystallographically characterized $Au_{102}(SR)_{44}$ cluster in 2007,[2,2] nanoclusters containing up to 333 Au atoms have been reported.[3] The stability of these clusters is explained with the "superatom" theory first described by Häkkinen and collaborators, which predicts structure based on closed electronic shell configurations.[1a, 4] This property differentiates "magic number" clusters from coordination clusters, the latter featuring Au(I) centers held together via aurophillic interactions and bridging X-type ligands.[5]

Thiols have long been the ligands of choice for superatom nanoclusters.[6] L-type ligands such as phosphines can also be employed, although these ligands are not as omnipresent as thiolates.[7] Clusters in which the only ligands are NHCs are limited to a handful of examples. In seminal work, Sadighi[8] and Bertrand[9] showed that mixed valence NHC clusters (Au(0/1)) can be prepared by reaction of carbon monoxide with Au carboxylates or μ_3-oxo Au clusters (Figure 1A). NHC-stabilized coordination clusters with gold atoms in the +1 state have been reported by Corrigan[5a] and Shionaya,[10] but thus far, there have been no examples of all-NHC magic number Au(0) nanoclusters. Considering the high activity of Au(0) clusters in catalysis[1c] biomedicine, sensing, imaging, optics and energy conversion[6b], and the rising interest in the use of NHCs as stabilizing ligands for metal surfaces,[11] access to these unique structures is of significant importance. Our groups recently succeeded in introducing NHCs into the known phosphine-stabilized Au_{11} nanoclusters via a ligand exchange approach (Figure 1B).[12] The number of NHCs introduced could be tuned in the range of 1–5, but complete replacement was not possible.

Herein we describe a straightforward, high yielding synthesis of gold (0) superatom clusters functionalized by all NHCs along with their structure determination by X-ray crystallography (Figure 1C). These clusters have unique photophysical properties, including among the highest quantum yields reported for gold nanoclusters.[13]

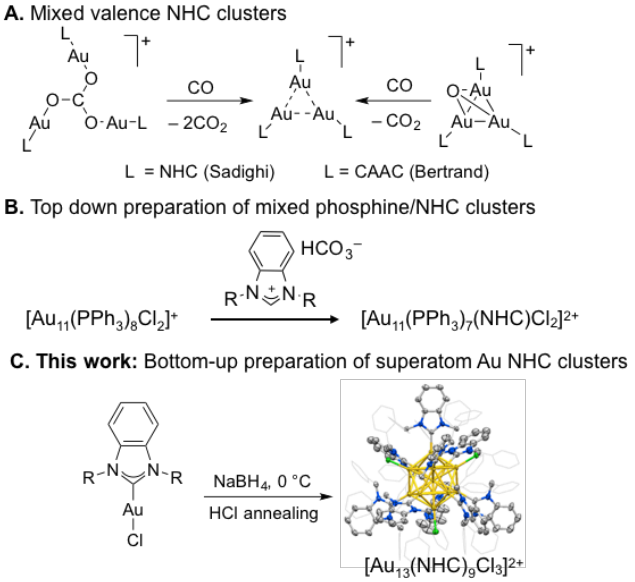

Figure 1: NHC-containing Au clusters. **A**: NHC-stabilized mixed valence Au(0/1) clusters; **B**: Mixed phosphine/NHC–stabilized Au(0) clusters; **C**: All NHC-stabilized Au(0) clusters.

We and others have previously shown that the wingtip groups on the NHC are of paramount importance in terms of bonding modes to planar gold surfaces.[11g, 11k, 14] In the synthesis of NHC-containing nanoclusters, we also showed that the nature of the NHC ligand had a large effect on the substitution chemistry, with benzyl substituents providing the cluster with the highest extent of NHC for phosphine subsitution.[12] In a key computational paper, Tang and Jiang[15] have predicted that aromatic wing–tip groups will provide considerable stabilization when NHCs bind to surfaces of all types, but that when unusually bulky NHCs are employed, the number that can be introduced around a gold core is limited.

In recent work from our group where a displacement reaction was used to prepare mixed NHC/phosphine gold clusters, we found that the use of benzylated NHCs gave the largest number of NHCs on the cluster under comparable conditions. Based on this, the Jiang predictions, and the likelihood of π-π interactions stabilizing the cluster, we targeted benzylated NHC **1a** as our first choice for the first de novo synthesis of Au–NHC nanoclusters.

Precursor synthesis began with the preparation of molecular NHC–Au–Cl complexes. In addition to benzimidazolium salt **1a**, we also examined related salts **1b-f**, which have aromatic substituents on the wing-tip groups. The desired gold complexes could be produced easily and in high yield by the reaction of commercially available Me_2S–Au–Cl with benzimidazolium salts (**1a-e**) in the presence of K_2CO_3, following the work of Nolan and co-workers for the preparation of related Au–NHC complexes (Equation 1).[16] The use of these simple complexes as starting materials for cluster synthesis already presents an advantage vs. thiolate chemistry, where reduction is performed on an ill-characterized and likely polymeric mixture of sulfur-bridged species.[6b]

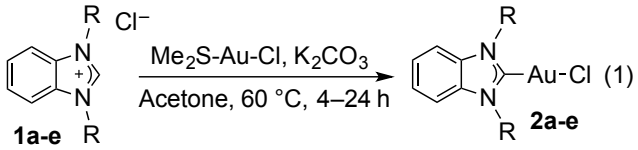

(a) R = Bn (b) R = CH_2(4-MeC_6H_4)
(c) R = CH_2(2-MeC_6H_4) (d) R = Ph (as BF_4 salt)
(e) R = CH_2(2-Np)

With NHC–Au–Cl complexes **2a-e** in hand, we optimized the conditions for cluster synthesis with **2a** using $NaBH_4$ as the reducing agent. Initial results were promising, with UV-vis data indicative of the presence of clusters rather than nanoparticles. After investigating a variety of conditions, we eventually settled on reduction at 0 °C, followed by warming to room temperature and treatment with HCl, taking inspiration from the work of Konishi on phosphine-Au clusters (Equation 2).[17]

Examining the clusters by UV-visible spectroscopy and ESI-MS before and after HCl treatment was highly instructive (see S.I.). ESI-MS analysis showed that even the crude material contained only molecular species and Au_{13} clusters, with no other significant cluster species detected. No significant changes were detected by ESI-MS after HCl treatment. The UV-vis spectra, however, were significantly sharper after HCl treatment (see S.I.). This suggests that the effect of HCl is not to focus cluster size, but rather to enhance the purity of the cluster in terms of ligand arrangement.[18]

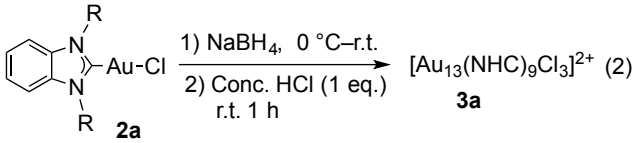

The molecular formula of the cluster was determined to be $[Au_{13}(NHC)_9Cl_3]^{2+}$, by ESI-MS analysis (Figure 2). This formula yields 8 delocalized electrons left in the gold core, in agreement with the predictions for an enhanced stability from the superatom theory,[3] and is also closely related to the cluster $[Au_{13}(NHC)_{10}Cl_2]^{3+}$ predicted by Tang and Jiang.[15]

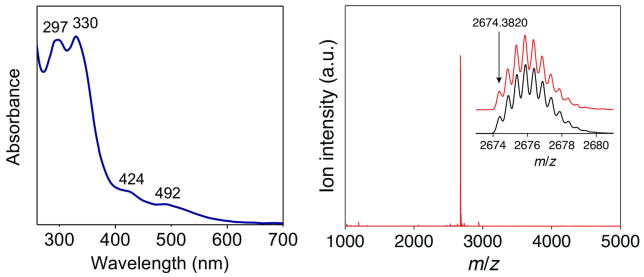

Figure 2: UV-vis spectrum (left) and ESI-MS (right) of [**3a**][PF_6]$_2$

Structural characterization of cluster **3a** was achieved by anion exchange to yield the related PF_6^- cluster, [**3a**][PF_6]$_2$, followed by crystallization from a supersaturated acetonitrile/diethyl ether solution. Under these conditions, single crystals of suitable quality for X-ray diffraction analysis were obtained. As shown in Figure 3, the cluster is comprised of an icosahedral Au_{13} core with one gold atom at the center, with the remaining gold atoms bound to either chloride or NHC ligands.

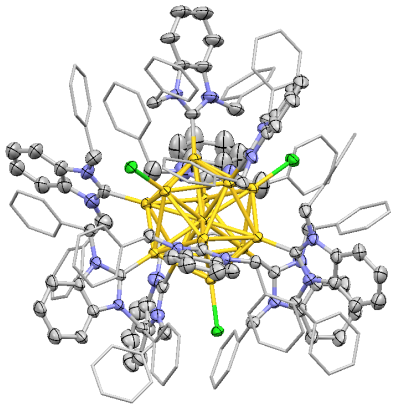

Figure 3: Molecular structure of [**3a**][PF_6]$_2$ with ellipsoids shown at 30% probability level. Anions and hydrogen atoms

have been removed, and phenyl rings from wingtip groups shown as wireframe for additional clarity. For additional representations, and all bond lengths and angles, please see Supporting Information. Colour key: carbon (grey); nitrogen (blue); chlorine (green); gold (yellow).

As expected, the NHCs are bound via a single Au–C bond, with Au-C and Au-Au bond lengths within expected values (For more details, see Supporting Information). In addition to providing clarity on the core Au structure, the X-ray crystallographic data also show the importance of interactions between the ligands. The cluster contains multiple CH–π and π-π interactions between the benzyl substituents and both rings of the benzannulated NHC core (see Supporting Information). The structural rigidity implicated by these interactions is likely responsible for the presence of long lived excited states (*vide infra*).

Through the use of ^{13}C labeled NHC precursors, we were able to identify the carbon-gold bonds as occurring in the 200–214 ppm range, consistent with the observation of the ^{13}C NMR signal for the single NHC in the mixed cluster $[Au_{11}(NHC)(PPh_3)_7Cl_2]Cl$ at 209 ppm.[12]

In order to test the generality of the cluster synthesis, and the importance of the benzyl groups, we subjected NHC–Au–Cl complexes **2b**-**2e** to the same reducing conditions followed by HCl treatment. The procedure was found to be general, but the clusters produced are highly sensitive to the steric constraints of the wingtip groups. For example, Au complex **2b**, in which methyl groups are introduced onto the para position of the benzyl groups, still gives Au_{13} clusters, as judged by UV-vis spectra and ESI–MS analysis. Complex **2c**, which contains an ortho methylated benzyl group, was also examined. This more hindered precursor gave slightly different clusters with the molecular formula $[Au_{13}(NHC^{oTol})_8Cl_4]^+$, accompanied by other species, indicating the significant effect of sterics. Consistent with this, aryl rings attached directly to the ring as in **2d** were completely ineffective, giving no nanoclusters and illustrating the importance of flexibility in the NHC wingtip groups. NaphthylCH_2– substituents were tolerated, with complex **2e** giving Au_{13} cluster **3e** in good yield.

With three new NHC-stabilized Au_{13} clusters in hand, we turned to a study of their properties. The thermal stability of the various clusters was assessed by heating acetonitrile solutions of the clusters while examining changes to their UV-vis spectra. For comparison, the all phosphine cluster $[Au_{11}(PPh_3)_8Cl_2]Cl$ (**4**)[19] was subjected to the same thermal treatment. As shown in Figure 4A, the all phosphine–protected cluster underwent full decomposition, while clusters **3a** and **3e** retained much of their initial colour. Further analysis by UV-vis spectroscopy (Figure 4, panels B-D) illustrated that phosphine cluster **4** completely decomposed after 4 hours. By comparison, all NHC-protected cluster **3a** showed only slight decomposition over the same time frame, and cluster **3e** shows virtually no decomposition (Figure 4, panel D).

This improved stability is consistent with TGA analysis of the clusters, which demonstrate some loss of ligand at 235 °C and complete desorption at 585 °C. In contrast, for cluster **4**, ligand loss begins at 150 °C and complete loss of ligand is complete at 245 °C (see S.I.).

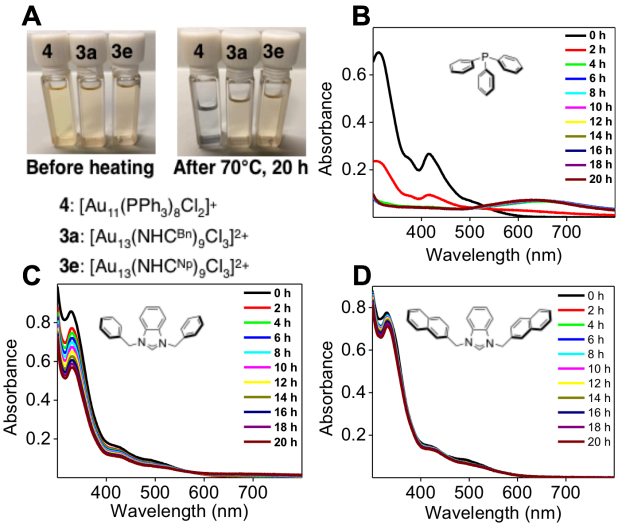

Figure 4: Study of Au clusters **4**, **3a** and **3e** before and after 20h of heating in acetonitrile at 70 °C. **A**: visuals of clusters before and after heating; **B**: UV-vis spectra of $[Au_{11}(PPh_3)_8Cl_2]Cl$ from 0-20h heating; **C** UV-vis spectra of $[Au_{13}(NHC^{Bn})_9Cl_3]^{2+}$ (**3a**) from 0-20h heating; **D** UV-vis spectra of $[Au_{13}(NHC^{Np})_9Cl_3]^{2+}$ (**3e**) from 0-20h heating.

The structural and electronic properties of **3a**, **3c**, and **3e** were examined by DFT, using the crystal structure of **3a** as a starting point (technical details in SI). The binding energy of the NHC ligand in **3a** evaluated from the PBE functional (1.99 eV) is about the same magnitude as a typical Au-SR bond, but being clearly higher than a typical Au-PR_3 bond (by about 1 eV). When van der Waals interactions in the ligand layer are accounted for (BEEF-vdW functional), the predicted Au-NHC bond strength increases to 2.62 eV in **3a**.

Compounds **3a**, **3c**, and **3e** all have a very similar HOMO-LUMO energy gap of about 2.0 eV, reflecting the expected electronic stability of the 8-electron configuration (Figures 5, S.I.). The Kohn-Sham orbitals near the Fermi level show distinct symmetry properties when projected to the I_h point group in the volume of the gold core (see S.I.). The HOMO, HOMO-1 and HOMO-2 states have triply degenerate T_{1u} symmetry corresponding to the *p*-type spherical orbitals as expected for an 8-electron superatom. The first few unoccupied states have H_g symmetry corresponding to five-fold degenerate *d*-states in spherical representation, Cl ligands break both the T_{1u} and H_g states by lowering the symmetry from the core-I_h to C_3.

The calculated UV-vis spectra of **3a**, **3c**, and **3e** were in good agreement with the experimental data concerning

the location of the optical gap and the few visible absorption peaks (see S.I.). The superatom electronic structure predicts dipole-allowed HOMO→LUMO as the lowest optical transition as also confirmed from the spectral analysis (see S.I.). We also examined the first excited states where an electron is excited from the HOMO to the LUMO state by forcing the occupation numbers accordingly in the spin-polarized DFT calculation and relaxing the system with the PBE functional. The excited states of **3a** and **3e** were 1.68 eV and 1.61 eV higher in energy compared to the ground state, respectively. These energies correspond to 738-770 nm in wave length, in a excellent agreement with the observed emission spectra as discussed next.

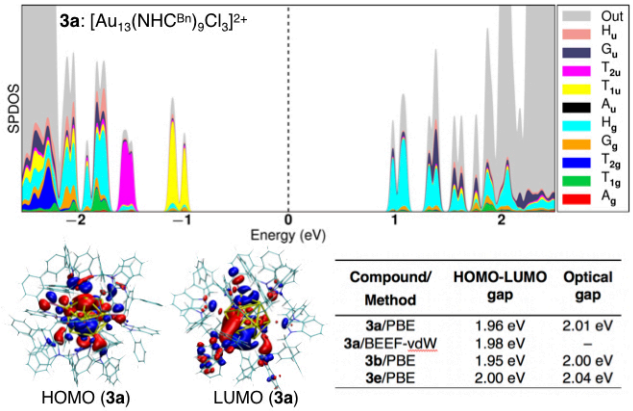

Compound/ Method	HOMO-LUMO gap	Optical gap
3a/PBE	1.96 eV	2.01 eV
3a/BEEF-vdW	1.98 eV	–
3b/PBE	1.95 eV	2.00 eV
3e/PBE	2.00 eV	2.04 eV

Figure 5: I_h symmetry-projected electronic density of states (SPDOS) of **3a.** Energy zero is at the center of the HOMO-LUMO gap. HOMO and LUMO orbitals are visualized.

Fluorescence excitation emission matrix (EEM) spectroscopy studies on **3e** are shown in Figure 6. Importantly, the excitation spectrum of **3e** matches very well with the absorbance spectrum for the same compound (Figure 4D). The quantum yield of fluorescence was also determined from EEM spectra (Figure 6B) with excitation matched to the standard, zinc phthalocyanine. Clusters **3e** and **3a** boast impressive emission quantum yields of 27% and 10%, respectively, making these some of the highest quantum yields ever recorded for gold clusters. The absorbance and/or emission onset can be used to estimate the HOMO/LUMO energy gap to be 616 nm (2.03 eV), in excellent agreement with DFT results (see S.I.), (see supporting information for more detailed analysis).[20] This is a further indicator of the purity of the clusters, and confirms that de-excitation of the superatom excited-state is responsible for the intense emission observed.[21]

In conclusion, we have reported the preparation of an all-NHC stabilized superatom Au_{13} cluster as a novel example of an 8-electron superatom with unusually high emission quantum yield and superior thermal stability to related phosphine-protected gold clusters.

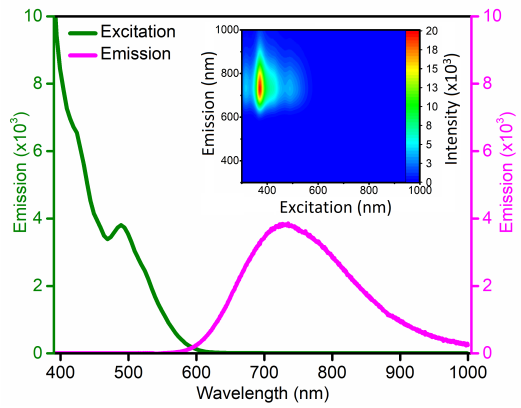

Figure 6. Fluorescence characterization of compound **3e**, Emission spectrum (with 420 nm excitation) and excitation spectrum (monitoring 730 nm emission) for **3e**. Inset: 3D EEM spectra of **3e**. illustrating the colour and the high quantum yield of emission under visible and UVA light.

AUTHOR INFORMATION

Corresponding Authors

*cruddenc@chem.queensu.ca
*hannu.j.hakkinen@jyu.fi
*tsukuda@chem.s.u-tokyo.ac.jp
*kevin.stamplecoskie@queensu.ca

ORCID

Hannu Häkkinen: 0000-0002-8558-5436
Tatsuya Tsukuda 0000-0002-0190-6379
Cathleen Crudden 0000-0003-2154-8107
Paul Lummis: 0000-0002-9212-3678

ACKNOWLEDGMENT

The Natural Sciences and Engineering Research Council of Canada (NSERC) and the Canada Foundation for Innovation (CFI) are thanked for financial support of this work in terms of operating and equipment grants to CMC and KS. MN thanks the Ontario government for an OGS fellowship and Mitacs–JSPS for funding to travel to Japan. HH thanks the Academy of Finland for support for Academy Professorship and CSC – the Finnish IT Center for Science for generous computers resources. SK thanks the Väisälä Foundation for a personal PhD study grant. This research was financially supported by the Elements Strategy Initiative for Catalysts & Batteries (ESICB) and a Grant-in-Aid for Scientific Research (A) (Grant No. 17H01182) from the Japan Society for the Promotion of Science (JSPS).

REFERENCES

1. (a) Häkkinen, H., *Nature Chem.* **2012,** *4*, 443; (b) Tsukuda, T.; Häkkinen, H., *Protected Metal Clusters: From Fundamentals to Applications* Elsevier: Amsterdam, 2015; (c) Yamazoe, S.; Koyasu, K.; Tsukuda, T., *Acc. Chem. Res.* **2014,** *47*, 816–824; (d) Li, G.; Jin, R., *Acc. Chem. Res.* **2013,** *46*, 1749–1758; (e) Bürgi, T., *Nanoscale* **2015,** *7*, 15553-15567.
2. Jadzinsky, P. D.; Calero, G.; Ackerson, C. J.; Bushnell, D. A.; Kornberg, R. D., *Science* **2007,** *318*, 430-433.

3. Zhou, M.; Zeng, C.; Chen, Y.; Zhao, S.; Sfeir, M. Y.; Zhu, M.; Jin, R., *Nature Commun*. **2016,** *7*, 13240.
4. (a) Häkkinen, H.; Walter, M.; Grönbeck, H., *J. Phys. Chem. B* **2006,** *110*, 9927-9931; (b) Walter, M.; Akola, J.; Lopez-Acevedo, O.; Jadzinsky, P. D.; Calero, G.; Ackerson, C. J.; Whetten, R. L.; Grönbeck, H.; Häkkinen, H., *Proc. Natl. Acad. Sci.* **2008,** *105*, 9157.
5. (a) Polgar, A. M.; Weigend, F.; Zhang, A.; Stillman, M. J.; Corrigan, J. F., *J. Am. Chem. Soc.* **2017,** *139*, 14045-14048; (b) Azizpoor Fard, M.; Levchenko, T. I.; Cadogan, C.; Humenny, W. J.; Corrigan, J. F., *Chem. Eur. J.* **2016,** *22*, 4543-4550; (c) Khalili Najafabadi, B.; Corrigan, J. F., *Dalton Trans.* **2014,** *43*, 2104-2111.
6. (a) Chakraborty, I.; Pradeep, T., *Chem. Rev.* **2017,** *117*, 8208-8271; (b) Jin, R.; Zeng, C.; Zhou, M.; Chen, Y., *Chem. Rev.* **2016,** *116*, 10346-10413.
7. (a) McKenzie, L. C.; Zaikova, T. O.; Hutchison, J. E., *J. Am. Chem. Soc.* **2014,** *136*, 13426-13435; (b) Konishi, K., *Struct. Bond.* **2014,** *161*, 49-86.
8. Robilotto, T. J.; Bacsa, J.; Gray, T. G.; Sadighi, J. P., *Angew. Chem., Int. Ed.* **2012,** *51*, 12077 –12080.
9. Jin, L.; Weinberger, D. S.; Melaimi, M.; Moore, C. E.; Rheingold, A. L.; Bertrand, G., *Angew. Chem., Int. Ed.* **2014,** *53*, 9059-9063.
10. Ube, H.; Zhang, Q.; Shionoya, M., *Organometallics* **2018,** *37*, 2007-2009.
11. (a) Crudden, C. M.; Horton, J. H.; Ebralidze, I. I.; Zenkina, O. V.; McLean, A. B.; Drevniok, B.; She, Z.; Kraatz, H. B.; Mosey, N. J.; Seki, T.; Keske, E. C.; Leake, J. D.; Rousina-Webb, A.; Wu, G., *Nature Chem.* **2014,** *6*, 409-414; (b) Crudden, C. M.; Horton, J. H.; Narouz, M. R.; Li, Z. J.; Smith, C. A.; Munro, K.; Baddeley, C. J.; Larrea, C. R.; Drevniok, B.; Thanabalasingam, B.; McLean, A. B.; Zenkina, O. V.; Ebralidze, I. I.; She, Z.; Kraatz, H. B.; Mosey, N. J.; Saunders, L. N.; Yagi, A., *Nature Commun.* **2016,** *7*, 1-7; (c) Zhukhovitskiy, A. V.; Mavros, M. G.; Van Voorhis, T.; Johnson, J. A., *J. Am. Chem. Soc.* **2013,** *135*, 7418-7421; (d) Zhukhovitskiy, A. V.; MacLeod, M. J.; Johnson, J. A., *Chem. Rev.* **2015,** *115*, 11503-11532; (e) Weidner, T.; Baio, J. E.; Mundstock, A.; Grosse, C.; Karthauser, S.; Bruhn, C.; Siemeling, U., *Aust. J. Chem.* **2011,** *64*, 1177-1179; (f) Engel, S.; Fritz, E.-C.; Ravoo, B. J., *Chem. Soc. Rev.* **2017,** *46*, 2057-2075; (g) Wang, G.; Rühling, A.; Amirjalayer, S.; Knor, M.; Ernst, J. B.; Richter, C.; Gao, H.-J.; Timmer, A.; Gao, H.-Y.; Doltsinis, N. L.; Glorius, F.; Fuchs, H., *Nat Chem* **2017,** *9*, 152-156; (h) Man, R. W. Y.; Li, C.-H.; MacLean, M. W. A.; Zenkina, O. V.; Zamora, M. T.; Saunders, L. N.; Rousina-Webb, A.; Nambo, M.; Crudden, C. M., *J. Am. Chem. Soc.* **2018,** *140*, 1576–1579; (i) Rühling, A.; Schaepe, K.; Rakers, L.; Vonhören, B.; Tegeder, P.; Ravoo, B. J.; Glorius, F., *Angew. Chem., Int. Ed.* **2016,** *55*, 5856-5860; (j) Salorinne, K.; Man, R. W. Y.; Li, C.-H.; Taki, M.; Nambo, M.; Crudden, C. M., *Angew. Chem., Int. Ed.* **2017,** *56*, 6198-6202; (k) Larrea, C. R.; Baddeley, C. J.; Narouz, M. R.; Mosey, N. J.; Horton, J. H.; Crudden, C. M., *ChemPhysChem* **2017,** *18*, 3536-3539.
12. Narouz, M. R. O., K. M.; Unsworth, P. J.; Man, R. W. Y.; Salorinne, K.; Takano, S.; Tomihara, R.; Kaappa, S.; Malola, S.; Dinh, C. T.; Padmos, J. D.; Ayoo, K.; Patrick, G. J.; Nambo, M.; Horton, J. H.; Sargent, E. H.; Häkkinen, H.; Tsukuda, T.; Crudden, C.M. *ChemRxiv Preprint* **2018**.
13. (a) Zheng, J.; Petty, J. T.; Dickson, R. M., *J. Am. Chem. Soc.* **2003,** *125*, 7780-7781; (b) Zheng, J.; Nicovich, P. R.; Dickson, R. M., *Annu. Rev. Phys. Chem.* **2007,** *58*, 409-431.
14. (a) Jiang, L.; Zhang, B.; Medard, G.; Seitsonen, A. P.; Haag, F.; Allegretti, F.; Reichert, J.; Kuster, B.; Barth, J. V.; Papageorgiou, A. C., *Chem. Sci.* **2017,** *8*, 8301-8308; (b) Kim, H. K.; Hyla, A. S.; Winget, P.; Li, H.; Wyss, C. M.; Jordan, A. J.; Larrain, F. A.; Sadighi, J. P.; Fuentes-Hernandez, C.; Kippelen, B.; Brédas, J.-L.; Barlow, S.; Marder, S. R., *Chem. Mater.* **2017,** *29*, 3403-3411; (c) Bakker, A.; Timmer, A.; Kolodzeiski, E.; Freitag, M.; Gao, H. Y.; Mönig, H.; Amirjalayer, S.; Glorius, F.; Fuchs, H., *J. Am. Chem. Soc.* **2018,** *140*, 11889-11892.
15. Tang, Q.; Jiang, D.-E., *Chem. Mater.* **2017,** *29*, 6908-6915.
16. Collado, A.; Gómez-Suárez, A.; Martin, A. R.; Slawin, A. M. Z.; Nolan, S. P., *Chem Commun* **2013,** *49*, 5541-5543.
17. Shichibu, Y.; Konishi, K., *Small* **2010,** *6*, 1216-1220.
18. Note we cannot rule out the influence of smaller or less stable clusters that do not survive ESI-MS analysis.
19. McKenzie, L. C.; Zaikova, T. O.; Hutchison, J. E., *J. Am. Chem. Soc.* **2014,** *136*, 13426-13435.
20. Tauc, J.; Grigorovici, R.; Vancu, A., *Phys. Status Solidi B* **1966,** *15*, 627-637.
21. Ramsay, H.; Simon, D.; Steele, E.; Hebert, A.; Oleschuk, R. D.; Stamplecoskie, K. G., *RSC Adv.* **2018,** *8*, 42080-42086.